O.M. PODOLYAN, T.V. ZAPOROZHETS, A.M. GUSAK

Bogdan Khmelnyts'kyi National University of Cherkasy
(81, Shevchenko Blvd., Cherkasy 18031, Ukraine; e-mail: ompodolyan@mail.ru)

PORE EVOLUTION AT REACTIVE DIFFUSION
IN SPHERICAL AND CYLINDRICAL NANOPARTICLES

A phenomenological model has been proposed for the description of the pore evolution at the phase formation in spherically and cylindrically symmetric binary systems "core–shell" with different mobilities of components. The dependences of the duration and the efficiency of the pore formation, relative pore stability, and degree of core restoration in the course of pore shrinkage on the initial dimensions of the system, surface tension, thermodynamic gain of formation/decay of a compound, and diffusion mobilities of components are analyzed. The ratio between the thermodynamic reaction gain and the surface tension is shown to be the governing parameter at the transition from the stage of nanoshell formation to that of its shrinkage; namely, it determines which of the regimes–pore formation and shrinkage with or without restoration of the initial components – will take place.

K e y w o r d s: void, nanoshell, diffusion, vacancies, reaction, Kirkendall effect, Gibbs–Thomson effect, intermediate phase

1. Introduction

The origin of the pore formation at the interface in a binary diffusion couple in the course of creation of solid solutions or compounds consists in different mobilities of components, which gives rise to the emergence of a compensating flux of vacancies opposite to the faster component flux. If the efficiency of vacancy sources or sinks is insufficient, the excess of vacancies, when exceeding the equilibrium concentration, is accumulated in pores (the Frenkel effect). This phenomenon is observed on the micro- [1, 2] and nanoscales [3–11] and near the planar [2,4] and curved interfaces (the interface "core–shell" with the spherical [1, 3, 5–8, 10, 11] or cylindrical [2, 4, 9] symmetry) of a diffusion couple. If the components are characterized by different diffusion mobilities, then, depending on the particle dimensions [5] and the temperature [6], the multipore formation or the centrally symmetric one with the emerging of hollow nanoshells and nanotubes becomes possible. For today, a variety of systems have been discovered, where the pore formation is accompanied by the formation of compounds (chalcogenides [3–9], intermetallic compounds [2]), or solid solutions of metals [1, 10, 11]. Several compounds rather than a single one can be formed – simultaneously or one by one – in the course of re-

actions. The appearance of additional (secondary) pores at the interfaces can be observed at that [9]. Almost right after hollow nanoshells had been experimentally fabricated, their instability [12, 13] – the shrinkage of shells under the influence of capillary phenomena without a possibility of their restoration – was predicted theoretically. However, the first experimental confirmations of the nanoparticle instability were obtained just for the case of restoration, when the hollow nanospheres of nickel and copper oxides shrinkaged and simultaneously transformed into solid particles of a pure metal. The shrinkage of oxides in air without restoration was confirmed only later [8].

The pore shrinkage, in its pure form, is a consequence of the Gibbs–Thomson effect (the difference between Laplace pressures). Restoration is a result of the chemical driving force. In nanoobjects, capillary and chemical forces can become comparable, and the corresponding processes can overlap. The characters of restoration and shrinkage, besides the ratio between the component mobilities, which is crucial at the formation stage, are also affected by the partial pressure of the external component (it is responsible for the capability of restoration and its extent) and the surface tension (it is the driving force of shrinkage). Depending on the relation between those parameters, either the simultaneous restoration and shrinkage of the shell or a sequence of those processes was experimentally observed [8, 9].
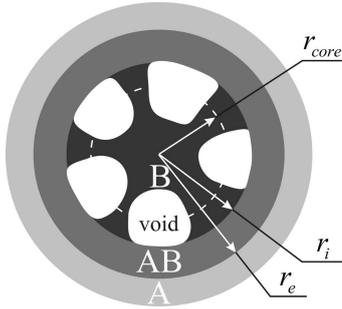
Fig. 1. Bridge model of pore nucleation and disappearance along the interface

The first model that described the shrinkage and took the possible restoration into account was proposed by us for the case of a solid solution in a wide interval of its homogeneity [14]. In this work, we propose, for the first time, to extend the model of shrinkage with restoration onto the case of a compound. For this purpose, we generalize the model of pore formation at the reactive diffusion [15] and consider the stages of pore formation and shrinkage, when one phase (a compound) with a narrow interval of homogeneity in the system "core B–shell A" emerges. The concept of "shell A" can correspond to one of three opportunities: (i) the solid layer of pure component A obtained as a result of the cladding, (ii) a mixture composed of component A with imbedded particles of component B, and (iii) a gas phase with a definite partial pressure of component A. Those variants are connected with different ways of the deliver of component A to the core consisting of component B. However, in the first case, the restoration to the initial geometry in the system "core–shell" is improbable, and the usage of the partial pressure concept is incorrect.

In order to describe the nucleation of a set of pores at the interphase boundary between the core and the formed compound, the "bridge model" [4] is used; namely, the bridges of a pure component survive between growing separated pores and serve as ways for the bulk and surface diffusions of a more mobile component from the core to the growing phase (Fig. 1). When the distance between neighbor pores (the bridge thickness) becomes comparable with the pore dimensions, the bulk diffusion through the direct bridge-to-phase contact becomes less effective than the surface diffusion along the bridge surface. The stage of shrinkage with simultaneous restoration of

component B can also be described in the framework of the same model, with the extraction of the islands of pure component B at the internal interface (hollow bridges between those islands necessarily survive up to the end of the shrinkage). Formally, the model describes the set of pores as a shell with an internal surface defined by the core radius r_{core} with regard for the volume of bridges and an external surface determined by the internal radius of the formed compound, r_i. A detailed analysis of the origin, driving forces, and mechanisms of pore formation/shrinkage, as well as the pore nucleation and stability, can be found in work [16].

2. Basic Assumptions and Model Equations

Let us unify the model equations as follows.

1. For specimens with various geometries (spherical and cylindrical), the surface (Laplace) energy per atom is defined as $E_{GT} = f\gamma\Omega/r_0$, where γ is the surface tension, Ω the atomic volume, r_0 the initial core radius, and $f = 2$ for spheres and 1 for cylinders.

2. For the description of both pore evolution stages (formation and shrinkage), the transition from the pore formation to its shrinkage is provided by changing the sign and the magnitude of the ratio $G^* = \Delta g/E_{GT}$ between the thermodynamic gain of a reaction per atom Δg (it corresponds to the energy gain at the mixing of components) and the surface energy E_{GT}.

Let us present some speculations concerning the application of the thermodynamic gain Δg. The stage of pore formation is connected with the emergence of a compensating flux of vacancies in the course of phase formation of a compound (an intermetallic compound or a chalcogenide denoted below as IMCs – intermediate compounds) with the thermodynamic driving force $\Delta g_{p_n}^{IMC} = g_{eq(p_n)}^{A+B} - g^{IMC}$, where g^{IMC} is the Gibbs potential per compound atom (i.e. the Gibbs free energy released per atom at the IMC formation from the mixture of components, provided that the conservation law of matter is obeyed), and $g_{eq(p_n)}^{A+B}$ is the Gibbs potential per atom in a mixture with the average concentration c^{IMC} (Fig. 2). It is evident that, for the IMC to be formed, it is necessary that the inequalities $g^{IMC} < g_{eq(p_n)}^{A+B} \Rightarrow \Delta g_{p_n}^{IMC} > 0$ should be satisfied (neglecting the curvature effect).

The system will proceed to the shrinkage stage if the initial components A and B are exhausted and/or

the vacancy flux is suppressed by the Laplace pressure. The majority of experiments known to the authors were carried out separately for the formation and shrinkage stages under varied external conditions [1–9]. D. Beke and collaborators revealed such systems and modes, when the both stages take place in the same experiment under fixed external conditions [10, 11].

For the component to be separated (the restoration of core component B), it is also necessary that the Gibbs potential for the compound should become less beneficial than that for the mechanical mixture of components with the same concentration, $g^{\text{IMC}} > g^{\text{A+B}}_{\text{eq}(p_n)}$. It can be achieved by increasing g^{IMC} – e.g., by changing to a different temperature regime, for the IMC, in accordance with the state diagram, to decay – or reducing the potentials of pure components. For instance, by reducing the partial pressure and, hence, the chemical potential of a volatile external component ($g^{\text{A}}_{p_r}$, Fig. 2), copper particles were experimentally obtained while annealing oxide shells in vacuum [8]. At the restoration (and, accordingly, at the change of gain sign, $\Delta g^{\text{IMC}}_{p_r} < 0$), the sign of the concentration gradient dc_{B}/dr in the compound changes to the opposite one (when the IMC is formed, the concentration of component B decreases at larger distances from the center, whereas the situation is inverse at the restoration of pure components). Experimentally, it is easier to monitor the variation of, e.g., the partial pressure p_r than the Gibbs potential $g^{\text{A}}_{p_r}$, because the ratio between the pressure p_r, at which the restoration is possible, and the atmospheric one, p_n, exponentially depends on the change of the Gibbs potential,

$$p_r/p_n = \exp\left(\frac{1}{kT}\left(g^{\text{A}}_{p_r} - g^{\text{A}}_{p_n}\right)\right).$$

We note that

$$g^{\text{A+B}}_{\text{eq}(p_n)} - g^{\text{A+B}}_{\text{eq}(p_r)} = \Delta g^{\text{IMC}}_{p_n} - \Delta g^{\text{A+B}}_{p_r}$$

and

$$g^{\text{A+B}}_{\text{eq}(p_n)} - g^{\text{A+B}}_{\text{eq}(p_r)} = \left(1 - c^{\text{IMC}}\right)\left(g^{\text{A}}_{p_n} - g^{\text{A}}_{p_r}\right).$$

Then, in case of the plane interface between the phases, for the transition to the restoration stage to take place at a constant temperature, it is necessary
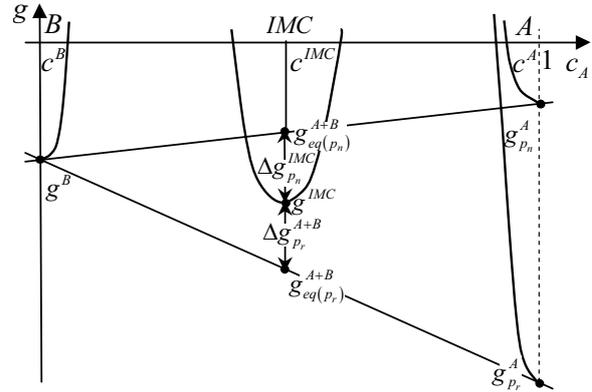
Fig. 2. Thermodynamic gains of the IMC formation from pure components A and B, $\Delta g^{\text{IMC}}_{p_n}$, and the restoration of components A and B, $\Delta g^{\text{A+B}}_{p_r}$. g^{IMC}, g^{B}, $g^{\text{A}}_{p_n}$, and $g^{\text{A}}_{p_r}$ are the Gibbs potentials per atom for the compound, pure component B, and pure component A at the normal and lowered pressures, respectively

that the partial pressure of oxygen be reduced down to p_r, and the thermodynamic gain

$$\Delta g^{\text{A+B}}_{p_r} = \Delta g^{\text{IMC}}_{p_n} + \left(1 - c^{\text{IMC}}\right) kT \ln\left(p_r/p_n\right)$$

become negative. For instance, in order to change the sign of the thermodynamic gain at the parameters used in this work, it is enough to diminish the partial pressure by a factor of four, and, to reach the effective shrinkage process with restoration, by a factor of ten (at $T = 500$ K, we have $c_B = 0.5$, $\Delta g^{\text{form}} = 5 \times 10^{-21}$ J, and $\Delta g^{\text{shr}} = -3.33 \times 10^{-21}$ J). Since we consider particles with a considerable curvature of their interphase boundaries, the phase equilibrium in them additionally depends on the Laplace pressure [15]. While taking its influence on the phase equilibrium into account, it is necessary to bear in mind that the Laplace pressure is nothing else but a jump, across the interface, of the stress tensor component normal to the interface (it is possible to make allowance for either the positive contribution $f\gamma\Omega/r$ for the phase outside the interface or the negative contribution $-f\gamma\Omega/r$ for the phase inside the interface). To make the derivation procedure simpler, it is convenient to add the negative term $-f\gamma\Omega/r_e$ to the Gibbs potential g^{A} of shell A and the positive term $+f\gamma\Omega/r_i$ to the Gibbs potential g^{B} of core B. Elementary geometrical reasonings allow one to determine the cumulative influence of two curvatures

on the gain $\Delta g_{p_r}^{\mathrm{A+B}}$,

$$\Delta g_{p_r}^{\mathrm{A+B}} = \Delta g_{p_n}^{\mathrm{IMC}} + \left(1 - c^{\mathrm{IMC}}\right) kT \ln \left(p_r/p_n\right) +$$

$$+ f\gamma\Omega \left(\frac{c^{\mathrm{IMC}}}{r_i} - \frac{1 - c^{\mathrm{IMC}}}{r_e}\right) < 0.$$

From this inequality, it is possible to estimate the required change of the partial pressure p_r/p_n for the restoration to begin.

Below, using the dimensionless parameter $G^* = \Delta g/E_{\mathrm{GT}}$, we use the common notation Δg for the thermodynamic gain, and its sign and magnitude determine the probability for the IMC to be formed or to decay.

While describing the kinetics of the process, we confine the consideration to the case of diffusion-controlled reaction at both formation and shrinkage stages. This means that the reaction time is mainly spent on the diffusive migration of components through the compound interlayer.

To describe the evolution of voids from nucleation to shrinkage, we draw three concentric boundaries (Fig. 1). The boundary at $r = r_{\mathrm{core}}$ confines the core (component B), and the boundaries at $r = r_i$ and $r = r_e$ the IMC shell. The pores that emerge inside the "core–IMC" interface are represented as a void with the volume equal to that of the shell between r_{core} and r_i. The available substance bridges between the core and the shell are diffusion paths and allow the flux balance equation at the internal boundary $r = r_i$ to be written down at the theoretical consideration. Since there is no component A in the core and no component B outside the IMC shell, we write down the flux balance across the internal boundary r_i for the former and across the external boundary r_e for the latter component. We also consider the contribution to the component fluxes made by the gradient of vacancy concentration that emerges between the curved external and internal boundaries as a result of the Gibbs–Thomson effect,

$$(0 - c_{\mathrm{B}}) \frac{dr_e}{dt} 0 - \left(-D_{\mathrm{B}} \frac{\partial c_{\mathrm{B}}}{\partial r}\bigg|_{r_e} + \frac{c_{\mathrm{B}} D_{\mathrm{B}}^*}{c_{\mathrm{V}}} \frac{\partial c_{\mathrm{V}}}{\partial r}\bigg|_{r_e}\right), \quad (1e)$$

$$(c_{\mathrm{A}} - 0) \frac{dr_i}{dt} = \left(-D_{\mathrm{A}} \frac{\partial c_{\mathrm{A}}}{\partial r}\bigg|_{r_i} + \frac{c_{\mathrm{A}} D_{\mathrm{A}}^*}{c_{\mathrm{V}}} \frac{\partial c_{\mathrm{V}}}{\partial r}\bigg|_{r_i}\right) - 0, \quad (1i)$$

where $D_{\mathrm{A}} = D_{\mathrm{A}}^* \phi$ and $D_{\mathrm{B}} = D_{\mathrm{B}}^* \phi$ are the partial diffusion coefficients of labeled atoms, $\phi = \frac{c_{\mathrm{A}} c_{\mathrm{B}}}{kT} \frac{\partial^2 g}{\partial c^2}$ is the thermodynamic factor, the diffusion coefficients of labeled atoms $D_{\mathrm{B}}^* = c_{\mathrm{V}} K_{\mathrm{B}}$ and $D_{\mathrm{A}}^* = c_{\mathrm{V}} K_{\mathrm{A}}$ are proportional to the vacancy concentration, and the partial coefficients of vacancies K_{B} and K_{A} are assumed constant in the framework of this model.

Since the component concentrations vary in a narrow interval of homogeneity for the atomic fractions of components in the compound ($\Delta c_{\mathrm{B}} = -\Delta c_{\mathrm{A}}$), we assume that $c_{\mathrm{B}} + c_{\mathrm{A}} \cong 1$ and $\frac{\partial c_{\mathrm{B}}}{\partial r} \cong -\frac{\partial c_{\mathrm{A}}}{\partial r}$. It should be noted that the fluxes are considered in the reference frame connected with the crystal lattice, the Kirkendall shifts are not taken into account, and the Manning correlation factors are also neglected, because they change the result only quantitatively. The flux equations (1) are rewritten as follows:

$$\frac{dr_i}{dt} = K_{\mathrm{A}} \left(\frac{c_{\mathrm{V}} \phi}{c_{\mathrm{A}}} \frac{\partial c_{\mathrm{B}}}{\partial r} + \frac{\partial c_{\mathrm{V}}}{\partial r}\right), \quad (2i)$$

$$\frac{dr_e}{dt} = K_{\mathrm{B}} \left(-\frac{c_{\mathrm{V}} \phi}{c_{\mathrm{B}}} \frac{\partial c_{\mathrm{B}}}{\partial r} + \frac{\partial c_{\mathrm{V}}}{\partial r}\right). \quad (2e)$$

We emphasize once more that, owing to the Gibbs–Thomson effect, the vacancy concentrations in Eqs. (2) at the external and internal interfaces can differ considerably, whereas the vacancy gradient does not tend to zero.

In compounds, the concentration is practically fixed by strong chemical bonds, so that the derivative of the concentration with respect to the time is close to zero at the points in the phase bulk. Therefore, for nearly stoichiometric compounds, we can apply the quasistationary approximation to both the components and the vacancies in the compound. From the continuity equation, we have

$$\frac{\partial c_{\mathrm{B}}}{\partial t} \approx 0 \Rightarrow \mathrm{div}\mathbf{J}_{\mathrm{B}} \approx 0,$$

$$\frac{\partial c_{\mathrm{V}}}{\partial t} \approx 0 \Rightarrow \mathrm{div}\mathbf{J}_{\mathrm{V}} + \sigma_{\mathrm{V}} \approx \mathrm{div}\mathbf{J}_{\mathrm{V}} \approx 0 \Rightarrow \mathrm{div}\mathbf{J}_{\mathrm{V}} \approx 0. \quad (3)$$

The powers σ_{V} of vacancy drains and sources in the specimen bulk are neglected, because the effective vacancy sources and drains are located only at the nanoshell surface, being absent from the newly formed phase [16]. Then, in the coordinate system of the lattice, the diffusion fluxes of vacancies, j_{V}, and

main components, j_B and j_A, are written down as follows taking the cross terms into account,

$$\mathrm{div} j_V \approx 0 \Rightarrow \frac{1}{r^f} \frac{\partial}{\partial r} \left(r^f j_V \right) \approx 0 \Rightarrow r^f j_V \approx \mathrm{const},$$
$$(4V)$$

$$r^f \Omega j_B (r) = r^f \left(-c_V (r) \phi \frac{\partial c_B}{\partial r} + c_B (r) \frac{\partial c_V}{\partial r} \right) \mathrm{K}_B =$$

$$= r_e^f \Omega j_B (r_e) = r_e^f \frac{dr_e}{dt} c_B, \qquad (4A)$$

$$r^f \Omega j_A (r) = r^f \left(-c_V (r) \phi \frac{\partial c_A}{\partial r} + c_A (r) \frac{\partial c_V}{\partial r} \right) \mathrm{K}_A =$$

$$= r_i^f \Omega j_A (r_i) = r_i^f \frac{dr_i}{dt} c_A, \qquad (4B)$$

where $\Omega j_A = \frac{dr_i}{dt} c_A$ and $\Omega j_B = \frac{dr_e}{dt} c_B$ are the fluxes of components A and B, respectively.

Equations (4A) and (4B) can be regarded as a system of two differential equations for two unknown functions, $c_B (r)$ and $c_V (r)$. Those equations are not linear, because the vacancy concentration $c_V (r)$ and the thermodynamic factor $\phi (r)$ cannot be put constant. However, the equations are linear with respect to the unknown quantities $\frac{dc_V}{dr}$ and $c_V (r) \phi (r) \frac{dc_B}{dr}$. After the corresponding transformations, we obtain the system of equations

$$\begin{cases} \dfrac{dc_V}{dr} = \dfrac{\mathrm{B}_1}{r^f}, \\ \phi (r) c_V (r) \dfrac{dc_B}{dr} = \dfrac{\mathrm{B}_2}{r^f}, \end{cases} \qquad (5)$$

where the parameters B_1 and B_2 are determined in terms of the interface motion velocities,

$$\begin{cases} \mathrm{B}_1 = r_e^f \dfrac{c_B}{\mathrm{K}_B} \dfrac{dr_e}{dt} + r_i^f \dfrac{c_A}{\mathrm{K}_A} \dfrac{dr_i}{dt}, \\ \mathrm{B}_2 = c_B c_A \left(\dfrac{r_i^f}{\mathrm{K}_A} \dfrac{dr_i}{dt} - \dfrac{r_e^f}{\mathrm{K}_B} \dfrac{dr_e}{dt} \right). \end{cases} \qquad (6)$$

After some mathematical transformations, we obtain the solutions for the cylindrical and spherical specimens;

$$\begin{cases} c_V (r) = \mathrm{B}_1 \ln |r| + F, \\ \phi (r) \dfrac{dc_B}{dr} = \dfrac{\mathrm{B}_2}{r (\mathrm{B}_1 \ln |r| + F)}, \end{cases} \qquad (7c)$$

$$\begin{cases} c_V (r) = -\dfrac{\mathrm{B}_1}{r} + F, \\ \phi (r) \dfrac{dc_B}{dr} = \dfrac{\mathrm{B}_2}{r^2 \left(-\frac{\mathrm{B}_1}{r} + F \right)}, \end{cases} \qquad (7s)$$

where F is the constant of integration. From the first equation in system (7c) with regard for the Gibbs–Thomson effect, we obtain the boundary conditions for the vacancy concentration at the external, r_e, and internal, r_i, interfaces,

$$\begin{cases} c_V (r_e) = c_{V0} \exp \left(-\dfrac{L_{\mathrm{GT}}}{r_e} \right), \\ c_V (r_i) = c_{V0} \exp \left(\dfrac{L_{\mathrm{GT}}}{r_i} \right), \end{cases} \qquad (8)$$

where c_{V0} is the equilibrium vacancy concentration in the bulk, and $L_{\mathrm{GT}} = \frac{f \gamma \Omega}{kT}$ is the characteristic Gibbs–Thomson length, which is determined by the surface energy at the curved surface.

Having integrated the second equation in system (5) over the radius from the internal to external interfaces [5], we obtain

$$\frac{\Delta g}{f \gamma \Omega} - \frac{\bar{c}_A}{r_e} + \frac{\bar{c}_B}{r_i} = \frac{\mathrm{B}_2}{\mathrm{B}_1} \left(\frac{1}{r_e} + \frac{1}{r_i} \right). \qquad (9)$$

Substituting expressions for B_1 and B_2, we obtain the equations for the motion velocities of shell boundaries,

$$\frac{dr_i}{dt} = -\mathrm{A} \frac{r_e}{r_e - r_i}, \quad \frac{dr_e}{dt} = \mathrm{B} \frac{r_i}{r_e - r_i}, \qquad (10s)$$

$$A = \frac{\mathrm{K}_A c_{V0}}{c_A} \frac{r_e}{r_i + r_e} \left(\frac{G^*}{r_0} + \frac{1}{r_i} \right) \times$$

$$\times \left(\exp \left(\frac{L_{\mathrm{GT}}}{r_i} \right) - \exp \left(-\frac{L_{\mathrm{GT}}}{r_e} \right) \right),$$

$$\mathrm{B} = \frac{\mathrm{K}_B c_{V0}}{c_B} \frac{r_i}{r_i + r_e} \left(\frac{G^*}{r_0} - \frac{1}{r_e} \right) \times$$

$$\times \left(\exp \left(\frac{L_{\mathrm{GT}}}{r_i} \right) - \exp \left(-\frac{L_{\mathrm{GT}}}{r_e} \right) \right).$$

Hence, the basic model equations are the equations for the motion velocities for the external, r_e, and internal, r_i, boundaries and the equation describing the change of the core radius (component B),

$$r_{\mathrm{core}} = \sqrt[f]{r_0^f - c_B \left(r_e^f - r_i^f \right)},$$
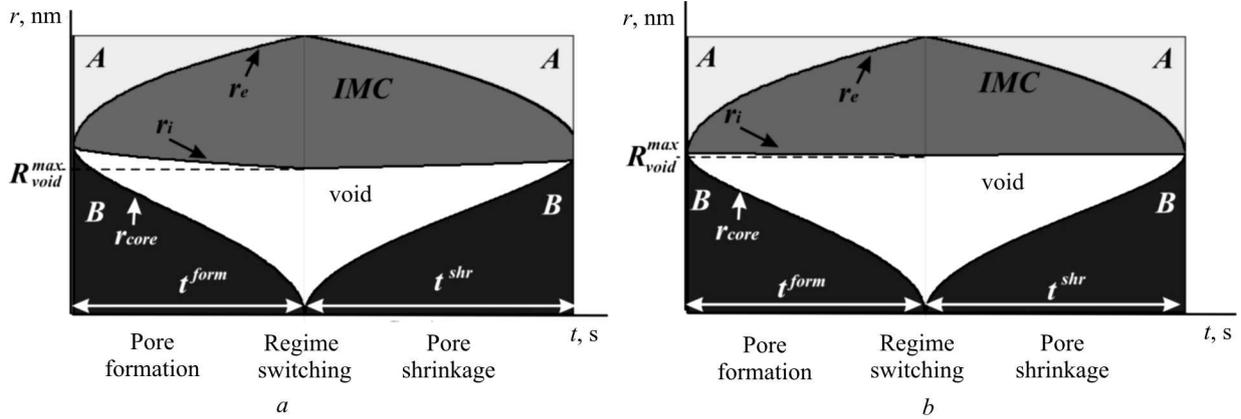
Fig. 3. Two consecutive stages of multipore formation and shrinkage at the core–IMC interface with (*a*) partial ($\kappa = 10$) and (*b*) complete ($\kappa = 100$) restoration. The pore volume is represented as a single void with the maximum dimension $R_{\text{void}}^{\max}$ at the time moment of exhaustion of component B and with the switching of regimes. The parameters are $r_0 = 1$ nm, $\gamma = 1$ J/m^2, $\Delta g^{\text{form}} = 5 \times 10^{-21}$ J, and $\Delta g^{\text{shr}} = -3.33 \times 10^{-21}$ J

which follows from the conservation law for pure component B in the core with the initial radius r_0.

3. Results and Discussion

At its initialization, the model system has a core (component B) with the radius r_0. Let us suppose that that the compound starts growing from the zero thickness, so that the initial internal and external radii of a IMC-shell are identical and equal to r_0. At the time moment, when the core totally disappears, $r_{\text{core}} \approx 0$, the process of phase formation comes to the end, and the pore reaches its maximum dimension $R_{\text{void}}^{\max} \approx r_i$ (Fig. 3). This time moment separates the formation stage with the duration t^{form} and the shrinkage one with the duration t^{shr} (it is also called "crossover" [16], if the both stages run under identical external conditions).

There exists an essential difference between the crossover in the case of mutual diffusion in a binary solid solution with the complete solubility (e.g., in the Ag–Au system in experiments by D. Beke and collaborators) and that in the case of reactive diffusion between mutually almost insoluble components with the formation and the growth of an intermediate compound with a narrow interval of homogeneity. In the case of solid solution, the transition from the formation stage to the shrinkage one should terminate *before* the complete homogenization, because the difference between the maximum and minimum concentrations at the boundaries and, hence, the corresponding

chemical force (the difference between the chemical potentials at the boundaries) supporting the fluxes of components and vacancies gradually decrease in the course of mutual diffusion. At a certain time moment, it cannot resist any more to the surface tension forces, which try to reverse the vacancy flux back inside. On the contrary, at the reactive diffusion between almost pure components, the driving force of the reaction per atom remains almost invariable up until one of the components is exhausted. Seemingly, the crossover should have occurred just at this time moment. However, the described scenario is too rough, because the force is determined not by a simple gain, but the gain divided by the shell thickness, which increases as the shell grows and reduces the force. Therefore, a certain dependence of the crossover on the gain could be expected, which is described below (Fig. 4)

In the model concerned, when changing from one stage to another one, the thermodynamic gain of IMC formation, which determines the energy benefit of the compound formation or decay, can also change. The criterion of the shrinkage stage termination is the disappearance of the pore, $r_{\text{core}} = r_i$. At this time momentum, initial components A and B can be partially ($r_{\text{core}} < r_{\text{core}0}$, Fig. 3,*a*) or completely ($r_{\text{core}} = r_{\text{core}0}$, Fig. 3,*b*) restored, depending on the ratio between the thermodynamic gain and the surface tension.

By numerically solving the obtained Eqs. (10), we analyzed the stages of pore formation and shrinkage at the temperature $T = 500$ K, the average shell concentration $c_{\text{B}} = 0.5$, the thermodynamic gains
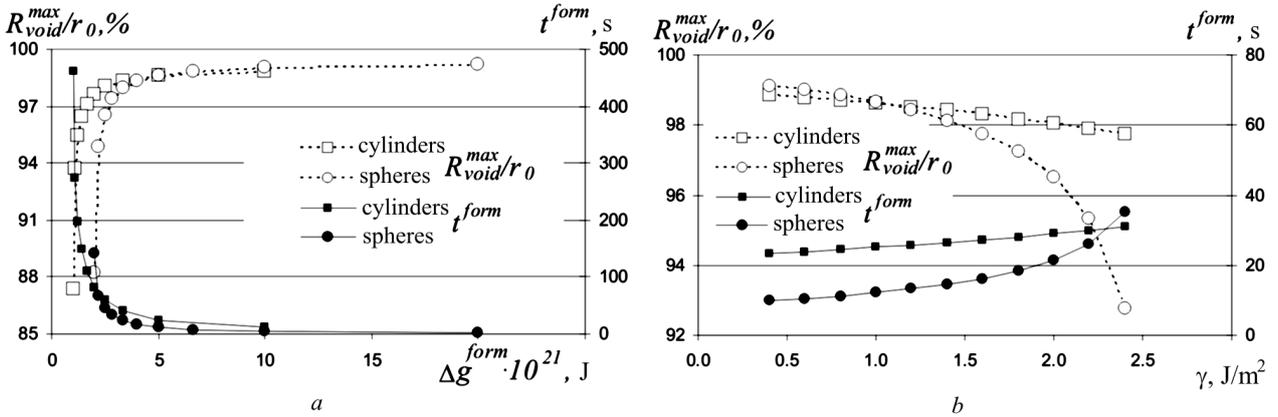
Fig. 4. Dependences of the efficiency, $R_{\mathrm{void}}^{\mathrm{max}}/r_0$, and the time, t^{form}, of pore formation on (*a*) the thermodynamic gain of phase formation Δg^{form} at $\gamma = 1$ J/m^2 and (*b*) the surface tension γ at $\Delta g^{\mathrm{form}} = 5 \times 10^{-21}$ J. The parameters are $c_B = 0.5$, $T = 500$ K, $\kappa = 100$, and $r_0 = 10$ nm

$\Delta g^{\mathrm{form}} = (10^{-21} \div 2 \times 10^{-20})$ J at the pore formation stage and $\Delta g^{\mathrm{shr}} = -3.33 \times 10^{-21}$ J at the shrinkage one, the dimensions of core (component B) in the interval $r_0 = 10 \div 50$ nm, the surface tension $\gamma = 0.4 \div 2.2$ J/m^2, and the component mobility ratio $\kappa = K_B/K_A = 2 \div 128$.

The efficiency of pore formation can be estimated as a degree of substitution of the initial core consisting of component B with the radius r_0 by a void with the radius $R_{\mathrm{void}}^{\mathrm{max}}$. If the thermodynamic gain of phase formation Δg^{form} increases, the maximum radius of a formed pore $R_{\mathrm{void}}^{\mathrm{max}}/r_0$ grows, by tending to an asymptotic value. The pore formation is more effective in cylinders at small gains and in spheres at larger ones (Fig. 4,*a*). The corresponding time of the maximum pore formation, t^{form}, decreases following the power law, as the gain increases, and, similarly to $R_{\mathrm{void}}^{\mathrm{max}}$, has a switching point. In other words, above a certain gain value, the pore formation becomes faster in spherical particles. The origin of this switching is the twice as large value of parameter L_{GT} for a spherically symmetric surface in comparison with a cylindrical one. The dependences of the radius of the maximum pore and the time of its formation on the surface tension γ also demonstrate a considerable reduction of the efficiency and the rate of pore formation in spherical particles with growing γ (Fig. 4,*b*).

If the mobility ratio κ increases, the pore radius $R_{\mathrm{void}}^{\mathrm{max}}$ can reach the size of the initial core, r_0. In other words, the more mobile component B of the core has enough time to diffuse into component A, which can do nothing else but "wait" for B to form a

compound with it. If the mobility of the core component increases, the time of the pore formation t^{form} decreases following the hyperbolic law $t^{\mathrm{form}} \sim 1/\kappa$, and the pore formation for spheres is faster than for cylinders.

A change of the initial core radius r_0 does not substantially affect the pore formation efficiency $R_{\mathrm{void}}^{\mathrm{max}}/r_0$, and the time of the maximum pore formation has a square-law dependence on the initial core radius for cylindrical particles and a power dependence with an exponent smaller than two for spherical ones.

A number of scenarios can be realized at the shrinkage stage (Fig. 5). They were observed experimentally [8] and analyzed theoretically for solutions [14] in following cases: shrinkage without restoration of the pure core component (C), shrinkage in vacuum with a complete or partial restoration of the core (C+B), and formation of the second phase enriched with the external component A (C+O), e.g., oxidation completion. Note, if the shrinkage is not followed by a complete restoration, the component separation is provided by another mechanism of mutual diffusion (taking the arising stresses into account). Therefore, this scenario of restoration after the shrinkage is not analyzed, being a subject of a separate research with a specification of the model. The scenario of the oxidation completion demands that the additional equations to describe the consecutive growth of two phases should be introduced into the model, which can also constitute a development of this model.
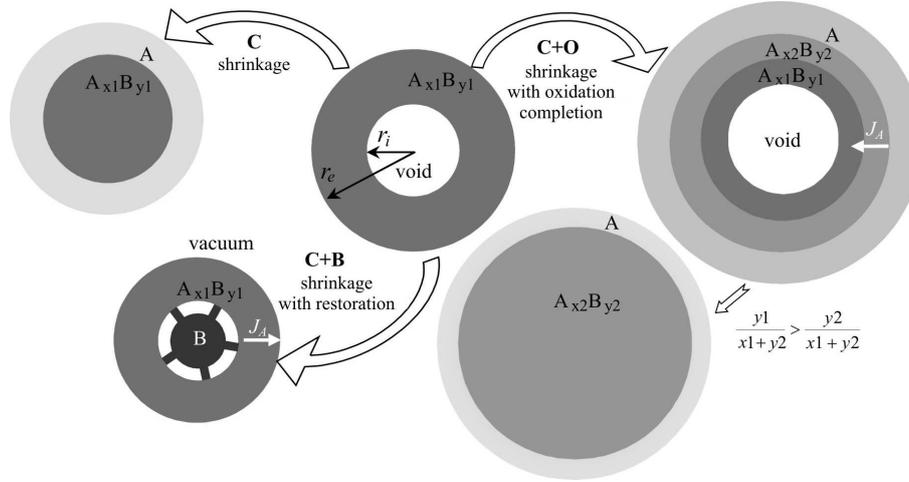
Fig. 5. Diagram of the hollow nanoshell shrinkage in vacuum (C+B) and air (C, C+O)
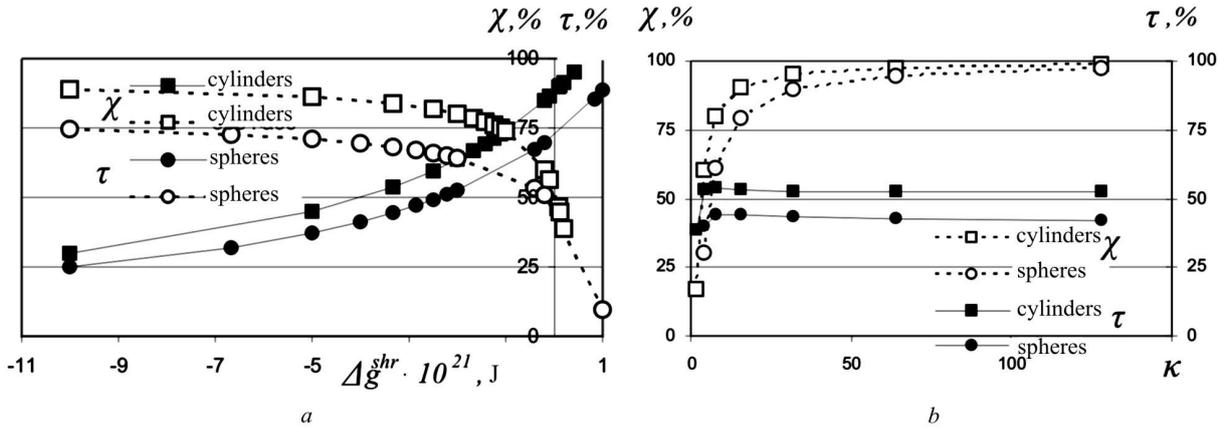
Fig. 6. Dependences of the restored fraction of core component B, χ, and the parameter of relative pore stability, τ, on (*a*) the thermodynamic gain of phase shrinkage Δg^{shr} at $\kappa = 10$ and (*b*) the ratio κ between the mobilities of components at $\Delta g^{\mathrm{shr}} = -3.33 \times 10^{-21}$ J. The parameters are $c_B = 0.5$, $T = 500$ K, $\gamma = 1$ J/m^2, and $r_0 = 10$ nm

For the quantitative estimation of the core restoration, we determined the fraction of restored component B, χ, at the time moment of the pore disappearance and the transformation of a nanoshell or nanotube into a nanoball or a nanowire,

$$\chi = 1 - \frac{c_{\mathrm{B}}\left(\left(r_e^{\mathrm{col}}\right)^f - \left(r_i^{\mathrm{col}}\right)^f\right)}{\left(r_0^{\mathrm{core}}\right)^f},$$

where r_i^{col} and r_e^{col} are the internal and external, respectively, radii of the rest of the non-restored IMC-shell at the time moment of the complete shrinkage (collapse) of a void.

If the negative thermodynamic gain, Δg^{shr}, decreases (its absolute value increases) at the stage of IMC-shell shrinkage, the fraction of the restored core component χ drastically grows and saturates at a certain value (Fig. 6,*a*). Such an asymptotic behavior becomes more pronounced if either the mobility ratio κ (Fig. 6,*b*) and/or the initial core dimension r_0 increase. The dependence of the increment of the restored core fraction χ on the surface tension, γ, reduction is almost linear. It is stronger for spheres, but is characterized by a less effective restoration. The complete restoration can be reached if either Δg^{shr} and γ simultaneously diminish or κ and r_0 simultaneously increase.

The formed shells are unstable as a result of the additional surface emergence, but can behave as metastable if the shrinkage time is much larger than the formation one [13]. For the quantitative estimation of stability, the parameter of relative stability of nanoshells, $\tau = t^{\mathrm{shr}}/\left(t^{\mathrm{form}} + t^{\mathrm{shr}}\right)$, calculated as the ratio between the shrinkage time t^{shr} and the total shell lifetime $t^{\mathrm{form}} + t^{\mathrm{shr}}$ – i.e. the closer is τ to 1, the more stable is the shell – was introduced. The shrinkage time and, accordingly, the relative pore stability may grow owing to the following factors: (i) a reduction of the thermodynamic gain of IMC decay at small absolute values of Δg^{shr} (Fig. 6,a), (ii) a reduction of the surface energy (small γ-values interfere less with the pore formation), and (iii) an increase of particle dimensions (large r_0-values make the curvature effects weaker).

The dependence of the relative stability τ on the ratio between the mobilities of the fast and slow components, κ, has a general tendency to grow, but reveals an insignificant nonmonotonic behavior – a drastic growth is followed by an insignificant recession – in a certain interval. A more detailed analysis of this nonmonotonicity (here, we do not discuss it) testifies that this feature is connected with the fact that shrinkage is accompanied by restoration. The competition between two factors takes place at that. On the one hand, an increase of the fast component mobility *accelerates* the restoration. On the other hand, the growth of the κ-ratio results in an increase of the segregation in the vacancy flux at the inverse Kirkendall effect, which *decelerates* the shrinkage [13].

Above, some cross-sections obtained at varying that or another parameter of the system (Δg, γ, r_0, κ) were analyzed, and the general tendencies for the main characteristics describing the stages of shell formation and shrinkage ($R_{\mathrm{void}}^{\max}/r_0$, t^{form}, χ, τ) were determined. The combined action of parameters can evidently strengthen or weaken that or another effect. For example, the complete restoration is possible at a negative thermodynamic gain, a reduction of particles, an increase in the surface tension, and a small difference between the component mobilities (Fig. 6,b).

In the course of mathematical description of the model, the dimensionless parameter $G^* = \Delta g/E_{\mathrm{GT}}$ was used, which was determined through a combination of the thermodynamic gain Δg, the surface tension γ, and the initial core radius r_0. The pore
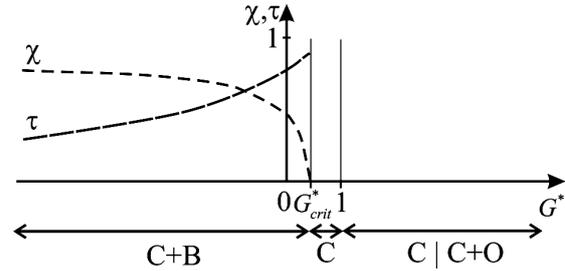
Fig. 7. Scenarios of the nanoshell shrinkage depending on the ratio $G^* = \Delta g/E_{\mathrm{GT}}$ between the thermodynamic gain at the restoration stage and the surface energy: shrinkage with possible restoration of components (C+B), without restoration (C), and with a possibility of the formation of another phase enriched with the external component (C+O)

formation occurs only if the thermodynamic gain Δg prevails over the Gibbs–Thomson energy, i.e. $G^* > 1$. However, if the phase shell already exists (being created under other conditions) and if the case $G^* < 1$ is realized, the shell shrinks, and this process can be accompanied by the restoration. A detailed analysis showed that separate intervals for the parameter G^* can be distinguished (Fig. 7), which determine the regimes of hollow nanoshell formation and shrinkage, as well as the possibility of shrinkage with restoration, according to scenarios depicted in Fig. 5.

Intuitively, we could predict that, in the interval $0 < G^* < 1$, the existence of IMC is thermodynamically beneficial, but the attempts of the system to minimize the surface energy would result in a gradual shrinkage (not so fast as if being accompanied by the restoration process). The carried out calculations showed that, in the interval $0 < G^* < G_{\mathrm{crit}}^*$, the shrinkage with restoration (scenario C+B, Fig. 6,a) does take place all the same, irrespective of the positive thermodynamic gain. This phenomenon has a kinetic rather than thermodynamic origin. Namely, a larger difference between the Laplace pressures results in a substantial vacancy flux into the shell, and a considerable difference between the component mobilities brings about the inverse Kirkendall effect, i.e. the segregation of components under the influence of the indicated vacancy flux. The segregation withdraws the compound composition beyond the limits of the homogeneity interval and induces a partial restoration of pure component B. In the interval $G_{\mathrm{crit}}^* < G^* < 1$, the shrinkage occurs under the influence of capillary forces, but the vacancy flux and, accordingly, the segregation degree in the inverse Kirk-

endall effect are already insufficient for the restoration, i.e. the compound remains in the homogeneity interval. In a vicinity of G^*_{crit}, the provisional and insignificant restoration is observed, which disappears afterward in the course of shrinkage, and no pure component B is extracted at the time moment of the pore collapse. The value of parameter G^*_{crit} depends on κ: the larger is κ, the closer to 1 is G^*_{crit}.

At $G^* > 1$, two shrinkage scenarios are possible for the already formed shell, depending on the state diagram of system A–B (Fig. 7). If the emergence of another phase, richer in component A, is possible in the system A–B, scenario C+O will be observed; otherwise, the process of shrinkage without restoration (scenario C) analyzed by us in work [13] in detail will take place.

It is very interesting to experimentally verify the possibility of the kinetically induced restoration in the interval $0 < G^* < G^*_{\text{crit}}$. The partial pressure of a reagent (e.g., oxygen at the formation and the shrinkage of oxides) can be a parameter to vary, which would provide achange of the thermodynamic gain Δg^{shr} together with G^*. In experiments by Nakamura *et al.* [8], only two points of our diagram depicted in Fig. 7 have been realized for today. These are the shrinkage of oxides without restoration in open air at a high temperature and the shrinkage with restoration in high vacuum.

4. Conclusions

One of the most promising applications of hollow nanospheres and nanotubes is the drug transport in a human body with the use of hollow nanocapsules (drug delivery). For such purposes, the most important characteristics are the maximum pore dimension and the nanoshell stability. As follows from the results of our research, for the pore dimension to be as large as possible, it is necessary that the diffusion coefficient of a slow component through the compound should be as low as possible, and the radius of the initial nanoparticle should be substantially larger than the critical one ($r_0 > f\gamma\Omega/\Delta g$), below which the capillary forces turn out more efficient than the chemical interaction related to the difference between the component mobilities.

A phenomenological model is developed, which allows the formation and the shrinkage of spherically or cylindrically symmetric hollow shells with a com-

plete or partial restoration to be described by varying the sign and/or the value of thermodynamic reaction gain. The model assumes the presence of the "core–phase" interface for supporting the paths ("bridges") for the delivery of a core substance to the reaction zone.

At the stage of hollow shell formation, the competing factors are, on the one hand, the thermodynamic benefit of the compound growth together with different partial diffusion coefficients of components and, on the other hand, the unprofitableness of the surface energy growth. This competition manifests itself more strongly for small particles with a substantial curvature effect.

A reduction of particle dimensions, increase in the surface energy, and growth of the thermodynamic gain of the compound decay (a decrease of the partial pressure of component A outside the shell or, in other words, an increase of the vacuum degree) reduce the stability of a nanoshell and favor its shrinkage. The dependence of the relative stability of a nanoshell on the ratio between the mobilities of components is non-monotonic and has a maximum. The fraction of the restored core substance at the time moment of the shell collapse is higher for larger particle dimensions, lower surface energy, larger absolute value of thermodynamic gain of the compound decay, and larger ratio between the component mobilities.

The partial restoration of components of a binary nanoshell is possible even if it is thermodynamically unprofitable. Namely, the extraction of the pure component can be a result of the kinetic effect, namely the inverse Kirkendall effect under the influence of the vacancy flux. The dimensionless parameter $G^* = \Delta g r_0 / f\gamma\Omega$ as a combination of three basic physical parameters of the model–the thermodynamic gain, surface tension, and particle size– governs which of the following regimes takes place: (i) formation of hollow shells ($1 < G^*$), (ii) shrinkage with restoration caused by the thermodynamic ($G^* < 0$, with the formation of "core B–shell A" structure) and kinetic ($0 < G^* < G^*_{\text{crit}}$) factors, and (iii) shrinkage of a nanoshell into a ball or a wire filled with the compound ($G^*_{\text{crit}} < G^* < 1$). The value of G^*_{crit} is determined by the fourth basic parameter of the model, namely, the ratio between the component mobilities, which competes with the thermodynamic benefit or unprofitableness for the compound to exist.

It is desirable to experimentally verify the existence of the interval of the partial pressure for the external component, at which the restoration occurs not owing to the thermodynamic benefit, but as a result of the segregation at the inverse Kirkendall effect beyond the limits of the phase homogeneity interval and the following phase decay. According to the results of our calculations, such a behavior has to manifest itself in the interval $0 < \Delta g r_0 / f \gamma \Omega < G^*_{\mathrm{crit}}$, where the value of G^*_{crit} is less than 1 and depends on the ratio between the diffusion coefficients of components.

1. F. Aldinger, Acta. Metall. **22**, 923 (1974).
2. Ya.E. Geguzin, *Diffusion Zone* (Nauka, Moscow, 1979) (in Russian).
3. Y. Yadong, R.M. Rioux , C.K. Erdonmez, S. Hughes, G.A. Somorjai, and A.P. Alivisatos, Science **304**, 711 (2004).
4. H.J. Fan, M. Knez, R. Scholz, D. Hesse, K. Nielsch, M. Zacharias, and U. Gosele, Nano Lett. **7**, 993 (2007).
5. C.M. Wang, D.R. Baer, L.E. Thomas, J.E. Amonette, J. Antony, Y. Qiang, and G. Duscher, J. Appl. Phys. **98**, 094308 (2005).
6. Y. Yin, C.K. Erdonmez, A. Cabot, S. Hughes, and A.P. Alivisatos, Adv. Funct. Mater. **16**, 1389 (2006).
7. A. Cabot, V.F. Puntes, E. Shevchenko, Y. Yin, L. Balcells, M.A. Marcus, S.M. Hughes, and A.P. Alivisatos, J. Am. Chem. Soc. **129**, 10358 (2007).
8. R. Nakamura, D. Tokozakura, J-G. Lee, H. Mori, and H. Nakajima, Acta Mater. **56**, 5276 (2008)
9. R. Nakamura, G. Matsubayashi, H. Tsuchiya, S. Fujimoto, and H. Nakajima, Acta Mater. **57**, 4261 (2009).
10. G. Glodán, C. Cserháti, I. Beszeda, and D.L. Beke, Appl. Phys. Lett. **97**, 113109 (2010).
11. G. Glodán, C. Cserháti, and D.L. Beke, Philos. Mag. **92**, 3806 (2012).
12. K.N. Tu and U. Gösele, Appl. Phys. Lett. **86**, 093111 (2005).
13. A.M. Gusak, T.V. Zaporozhets, K.N. Tu, and U. Gösele, Philos. Mag. **85**, 4445 (2005).
14. T.V. Zaporozhets, O.M. Podolyan, and A.M. Gusak, Metallofiz. Noveish. Tekhnol. **34**, 111 (2012).
15. A.M. Gusak and K.N. Tu, Acta Mater. **57**, 3367 (2009).
16. T.V. Zaporozhets, A.M. Gusak, and O.N. Podolyan, Usp. Fiz. Metall. **12**, 1 (2011).

О.М. Подолян, Т.В. Запорожець, А.М. Гусак

ЕВОЛЮЦІЯ ПОР ПРИ РЕАКЦІЙНІЙ ДИФУЗІЇ
У СФЕРИЧНИХ І ЦИЛІНДРИЧНИХ
НАНОЧАСТИНКАХ

Р е з ю м е

Запропоновано феноменологічну модель для опису еволюції пор при фазоутворенні у сферично і циліндрично симетричних бінарних системах "ядро|оболонка" з різною рухливістю компонентів. Проаналізовано залежність часу й ефективності пороутворення, відносної стійкості пор, а також ступеня відновлення ядра у процесі стягування від початкових розмірів системи, поверхневого натягу, термодинамічного стимулу утворення/розпаду сполуки, дифузійних рухливостей. Показано, що відношення термодинамічного стимулу реакції до поверхневого натягу є контролюючим при переході від стадії формування до стадії стягування нанооболонок – воно визначає режими утворення, стягування без відновлення або з відновленням вихідних компонентів.